MCB Accepts, published online ahead of print on 12 November 2012
Mol. Cell. Biol. doi:10.1128/MCB.00922-12

The SnAC domain of SWI/SNF is a histone anchor required for remodeling

Payel Sen[1,5], Paula Vivas[2], Mekonnen Lemma Dechassa[1,6], Alex M. Mooney[2], Michael G. Poirier[2,3,4] and Blaine Bartholomew[1#]

[1]Department of Biochemistry and Molecular Biology, Southern Illinois University School of Medicine, Neckers Building, Carbondale, IL 62901-4413, USA

[2]Department of Physics, [3]Department of Biochemistry and [4]Department of Molecular Immunology, Virology and Medical Genetics, Ohio State University, 1040 Physics Research Building, 191 West Woodruff Avenue, Columbus, Ohio 43210-1117, USA

Running Title: SnAC domain of SWI/SNF is a histone anchor

Word Count of Materials and Methods: 2004

Word Count of Introduction, Results and Discussion: 4642

[5]Present address: Department of Cell and Developmental Biology, University of Pennsylvania, 1051 BRBII/III, 421 Curie Boulevard, Philadelphia, PA 19104-6058, USA

[6]Present address: Colorado State University Department of Biochemistry and Molecular Biology, 1385 Center Avenue, Fort Collins, CO 80523, USA

#To whom correspondence should be addressed: bbartholomew@siumed.edu

Abstract

The SWI/SNF chromatin remodeling complex changes the positions where nucleosomes are bound to DNA, exchanges out histone dimers, and disassembles nucleosomes. All of these activities depend on ATP hydrolysis by the catalytic subunit Snf2 containing a DNA-dependent ATPase domain. Here we examine the role of another domain in Snf2 called SnAC (Snf2 ATP Coupling) that was shown previously to regulate the ATPase activity of SWI/SNF. We have found that SnAC has another function besides regulating the ATPase activity that is even more critical for nucleosome remodeling by SWI/SNF. We have found that deletion of the SnAC domain strongly uncouples ATP hydrolysis from nucleosome movement. Deletion of SnAC does not adversely affect the rate, processivity, or pulling force of SWI/SNF to translocate along free DNA in an ATP-dependent manner. The uncoupling of ATP hydrolysis from nucleosome movement is shown to be due to loss of SnAC binding to the histone surface of nucleosomes. While the SnAC domain targets both the ATPase domain and histones, the SnAC domain as a histone anchor is more critical role in remodeling because it is required to convert DNA translocation into nucleosome movement.

(187 words)

Introduction

Packing DNA into chromatin involves wrapping 147 bp of DNA around a histone octamer to form a nucleosome and nucleosomes are assembled into higher-order structures. Chromatin makes genomic DNA less accessible to protein factors important for transcription, replication, repair and recombination. Chromatin structure is dynamic due to remodeling factors, some of which are ATP-dependent that facilitate making discrete regions accessible to other factors. ATP-dependent chromatin remodelers are single or large multi-subunit assemblies composed of 1-17 subunits ranging from several kilodaltons to over a megadalton in molecular weight(5, 14). Each has a catalytic subunit with a conserved ATPase domain related to that of ATP-dependent DNA helicases. In helicases this domain couples ATP hydrolysis to DNA translocation and subsequent unwinding of double-stranded nucleic acid substrates by means of a translocase domain and a duplex destabilizing wedge domain(12, 15, 33). Unlike helicases, chromatin remodelers do not have nucleic acid unwinding activity, but have retained the translocase activity which in turn repositions or disassembles nucleosomes(29, 33).

Nucleosome movement by SWI/SNF and ISWI type complexes requires the ATPase domain to translocate along nucleosomal DNA near the dyad axis (6, 9, 30, 45). DNA gaps near the Superhelical Location (SHL) 2 of the nucleosome block movement without interfering with binding of the remodeler. DNA translocation this far inside of nucleosomes is challenging because there is no easy path for the ATPase domain to initially move. As the ATPase domain begins to translocate it encounters histone-DNA interactions in both directions and have to overcome multiple histone-DNA interactions while trying to pull DNA into nucleosomes. The force required to disrupt histone-DNA interactions as shown by mechanically unwrapping nucleosomes is ~23 pN and is a substantial force opposing the ATPase domain (1). SWI/SNF on the other hand was able to move nucleosomes against the inherent resistance of the

nucleosomes plus an opposing mechanical force of ~12 pN, which suggests that these enzymes could have a pulling force of >30 pN. And yet the ATPase domain alone does not appear to have a pulling force of 12 or 30 pN on free DNA and instead a mechanical force of only ~1pN is required to stall SWI/SNF and RSC translocation on free DNA. Presumably the intrinsic pulling force of the ATPase domain should be the same in either case. The ATPase domain may have greater tendency to "slip" on DNA tthan nucleosomes and a sufficient anchor to DNA is missing to prevent it from slipping. Evidence for tethering to the substrate being critical comes from a minimal complex of Arp7, Arp9, and a Tet dimer fused to a truncated copy of the catalytic subunit of RSC. This minimal complex can generate pulling forces of up to ~30 pN due to the tight binding of the Tet dimer to its recognition site (34) and is much higher than that observed for the native RSC complex. The questions remain for SWI/SNF and RSC as to the nature of the anchor in the native complex, whether DNA or histones are the targets, and the protein domain(s) that serves as anchor.

Many of the interactions of SWI/SNF with nucleosomes are not through nucleosomal DNA but with the face of the histone octamer not bound to DNA and are likely important for remodeling. The interactions of SWI/SNF with nucleosomes have been probed by site-directed crosslinking to specific sites in DNA and histones. DNA crosslinking has shown that Snf2, the catalytic subunit of SWI/SNF, is exclusively associated with nucleosomal DNA near SHL2 and other subunits are not seen elsewhere with extranucleosomal or nucleosomal DNA(9, 10). The only exception was the Snf6 subunit that is co-localized with the transcription activator Gal4-VP16 to its binding site in the extranucleosomal DNA region. In contrast SWI/SNF extensively interacts with the part of the histone octamer not bound by DNA in nucleosomes. Four subunits of SWI/SNF were crosslinked to segments of the H3-H4 tetramer and H2A-H2B dimer with Snf2 being one of the subunits most readily crosslinked(10). It seems likely the critical anchor for SWI/SNF is histones rather than DNA. Furthermore, DNA does not seem to be the

likely anchor given that SWI/SNF does not require extranucleosomal or nucleosomal DNA except that bound by the ATPase domain to move nucleosomes.

A domain in SWI/SNF that interacts with histones was identified in this study by tethering to histones a proteolytic agent that cleaves peptide bonds with hydroxyl free radicals similar to other studies using Fe-EDTA tethered to DNA or protein for mapping protein-DNA and protein-protein interactions (7, 8). Previously this approach has shown that the ATPase and HSA domains of Snf2 associate with free DNA when SWI/SNF is bound and identified the specific orientation of the ATPase domain relative to DNA (9). We now find the SnAC and ATPase domains are associated with the histone proteins when SWI/SNF is bound to nucleosomes. Our previous studies showed that the SnAC (Snf2 ATP Coupling) domain of Snf2 in yeast SWI/SNF is required for the ATPase and remodeling activities of SWI/SNF, but not for complex integrity, substrate recognition or recruitment function (31).

We found that without SnAC as the anchor domain ATP hydrolysis and DNA translocation activities are uncoupled from nucleosome mobilization by SWI/SNF. Deletion of the SnAC anchor domain diminished the interactions of SWI/SNF with the histone octamer, but not those with nucleosomal DNA. DNA movement inside the nucleosome is highly sensitive to the loss of the SnAC while translocation on free DNA is not either in terms of rate of movement, processivity, or pulling force.

Materials and Methods

Nucleosome reconstitution, gel shift assays for binding and remodeling

Mononucleosomes were reconstituted with 5.2 µg of PCR generated DNA from p-159-1 plasmid that had 29 and 59 bp of DNA flanking either side of the 601 nucleosome positioning sequence (29N59) or

with 8 µg of sonicated salmon sperm DNA, 100 fmoles ^{32}P labeled 29N59 DNA and 9 µg wild type *Xenopus laevis* octamer at 37°C by a rapid salt dilution method(3, 19). The labeled DNA was generated by PCR with an oligonucleotide labeled using Optikinase (USB) and [γ^{32}P] ATP (6000Ci/mole).

SWI/SNF complexes were purified as described previously (10). SWI/SNF was prebound to 29N59 nucleosomes (2.5 nM) containing only PCR-generated DNA at a molar ratio of 3:1 (full-binding conditions) for 15 min at 30°C and an additional 15 min at 25°C for measuring rates of nucleosome movement. ATP was added to a final concentration of 320 µM for ΔSnAC SWI/SNF or 4.4 µM for WT SWI/SNF) for different times, stopped and SWI/SNF competed off by addition of γ-thio ATP and salmon sperm DNA to a final concentration of 4.5 mM and 0.45mg/ml respectively. The remodeled products were analyzed on 5% native polyacrylamide gels (acrylamide:bisacrylamide=60:1) at 200V in 0.5X Tris-Borate-EDTA.

ATPase assays

ATPase kinetic assays were performed under conditions identical to remodeling kinetics with 0.055µCi γP^{32} ATP in a 13.5µl reaction volume.

Site-directed mapping

A unique cysteine was engineered at H2A 45 position by site-directed mutagenesis, overexpressed and purified as described (20). The histone mutant was refolded into octamer with WT H2B, H3 and H4. The mutant octamer was reconstituted into 29N59 nucleosomes with 1-4 pmoles of labeled DNA. In the nucleosome structure, H2A45 is in close proximity to one strand of nucleosomal DNA 37-39 bp from the dyad axis. After UV crosslinking, DNA scission is initiated at the crosslinked site by alkaline conditions. Para azido phenacyl bromide (APB) (Fluka) was added to 60 µl of reconstituted nucleosomes to a final

concentration of 400μM and incubated at 25°C for 3 hrs for conjugation of H2A 45. Remodeling time courses were performed with reaction volumes scaled up a factor of five, stopped by addition of γ-thio ATP and UV irradiated for 3 min at 312 nm. Samples were denatured with 0.1% SDS for 20 min at 70˚C and histone-DNA cross-linked samples purified by phenol-chloroform (4:1) extraction. The inter-phase containing the conjugates was washed three times with 1% SDS, 1M Tris-HCl pH 8.0 and precipitated with sodium acetate and ethanol. After washing the pellet with 70% ethanol, it was dried and resuspended in cleavage buffer (2%SDS, 20mM ammonium acetate, 0.1mM EDTA). DNA was cleaved at the cross-linked site by incubation in 0.1 M NaOH, for 45 min at 90˚C. The cleaved sample was neutralized with 2 M HCl and ethanol precipitated. Samples were resuspended in formamide and resolved on a 6.5% PAGE, containing 8 M urea and visualized by phosphorimaging.

DNA cross-linking

Probe synthesis was performed with *p*-azidophenacyl bromide (APB) modified phosphorothioate oligos that were radiolabeled close to the modification site with Optikinase (USB) and [γ^{32}P] ATP(27, 32). A series of modified oligonucleotides (IDT DNA) with the phosphorothioate located between the third and fourth nucleotides from the 5' end of the oligonucleotide were designed to scan the extranucleosomal (every 3 bp) and nucleosomal regions (every ~5 bp). Nucleosomes containing salmon sperm DNA and labeled probe were reconstituted and photocrosslinked with SWI/SNF recruited by Gal4-VP16 as described previously(26, 27, 32). Histone cross-linking was performed as described previously (10) using SWI/SNF purified from PSY2 and PSY3 (31). The intensity of the crosslinked band of interest was normalized to the H3 80 Snf2 signal in absence of ATP to find the relative crosslinking efficiency.

Single molecule DNA translocation assays

The DNA used in the single molecule experiments was a linearized 2.88 kb plasmid that contained a single asymmetric BsaI site on the opposite side of the plasmid from two Gal4 binding sites separated by 27 bp from a 601 high affinity nucleosome positioning sequence. The plasmid was linearized by BsaI and ligated to two short duplex DNA molecules, which contained the 4 bp single strand overhang that was complimentary to one of the two single stand overhangs created by the BsaI restriction enzyme. The two short dsDNA molecules were labeled with either biotin or digoxigenin. The 4 bp overhang that is created by BsaI is asymmetric. This ensures that the ligated linearized plasmid contained a biotin and digoxigenin at opposite ends. The biotin-labeled end of the DNA molecule was attached to a commercial super-paramagnetic bead (Dyna M280, Invitrogen) previously functionalized with streptavidin protein. The digoxigenin-labeled end was bound to a functionalized glass surface coated with anti-digoxigenin.

Our magnetic tweezers setup was similar to the one described by Strick et al (36, 37). Experiments were carried out in a lab built flow cells placed on a stage above a 60X oil-immersion lens mounted on an inverted microscope. The magnetic field used to manipulate the magnetic bead was generated by two magnets. The force on the DNA was determined from the thermal fluctuations of the tethered bead in the x-y plane and the distance between the bead and the glass surface via the equipartition theorem $F = k_B Tl / \langle \Delta x^2 \rangle$. Data acquisition was achieved using Labview image analysis software. The program tracks the position of the bead to determine the force being applied to the DNA and the distance between the bead and the glass surface. The DNA extension can be determined with an error of ~10 nm. The force was measured with 5-10 % accuracy. To eliminate the effects of microscope drift, differential tracking was performed by monitoring at the same time a second polystyrene bead glued to the surface. Data were acquired using 5nM WT SWI/SNF or 5nM SnAC mutant and 0.25 nM Gal4-VP16 protein. The reaction buffer was 20 mM Hepes (pH =7.8), 3 mM MgCl2, 0.08%NP-40, 0.2 mM PMSF, 2 mM BME, 53 mM NaCl, 0.02% Tween-20, 0.1 mg/ml BSA.

Nucleosome reconstitutions for single molecule nucleosome remodeling measurements.

Nucleosomes were reconstituted by salt double-dialysis(16, 40) in 50 µL volume with 0.1 µg of 2.9 kbp biotin-digoxigenin labeled DNA plasmid, 1.0 µg of 250bp containing the 601 DNA high affinity nucleosome positioning sequence, 2 µg of 147 bp low affinity DNA, 2 M NaCl, 1 mM benzamidine hydrochloride, 5 mM Tris-HCl (pH 8.0), and 0.5 mM EDTA. Samples were titrated with different amounts of histone of octamer, ranging from 1 to 3 µg, to find conditions where most of the tethers only have "1" or "0" nucleosomes. The histone octamer was prepared as previously described (23). Nucleosomes were characterized on a 5% acrylamide gel. The sample containing 1.6 µg histone octamer was used for most of the experiments presented here. This sample showed that on an average 20-30% of the tested molecules have one nucleosome.

Magnetic tweezers single molecule nucleosome remodeling measurements

The nucleosome sample was pre-incubated with streptavidin-coated magnetic beads (Dynabead M280, Invitrogen) at a ratio of 1:2 for 20 min in 20 µl of 0.5X TE with 0.1 mg/mL BSA for 20 min. The sample was injected into the flow cell (assembled with an antidigoxigenin-coated cover glass slide) at 2 µl/s and incubated for 10 min. Before the protein is added into the flow cell, the height of the DNA was recorded as a function of time for around 300 s and at constant force of 3 pN using a lab-built magnetic tweezers apparatus. Finally, 5 nM WT or ΔSnAC SWI/SNF protein and 1 mM ATP was flowed in. Addition of 0.5 nM Gal4-VP16 protein increased the probability of observing an event in a 5-10 min period. The height of the DNA in presence of the protein was recorded for ~300 s. Buffer conditions were identical to that described for the DNA experiments

We determined the number of nucleosomes within a single nucleosome sample by detecting the number of steps in the tether extension as the force was increased from 3 to 26 pN. The force was initially increased to 3 pN over 20 s, then increased from 3 to 26pN over 100 s, and then held at 26 pN for 250s. As an additional control the force was reduced to 0.3 pN and the height of the DNA was again tracked for ~300 s. This last control determines if the protein was active during the measurement and whether or not the sample contained one or zero nucleosomes.

A total of 27 remodeling events were analyzed independently. Based on the Brownian fluctuations, an 80 ± 10 bp threshold was set for determining the change in extension of a DNA molecule due to its interaction with SWI/SNF. Rates were estimated by analyzing each individual remodeling event. The shortening rates were fitted using straight lines with an average of 100 ± 50 bp/s. The average time of the remodeling event was estimated to be 20 ± 10 s.

Conjugation of Fe-BABE to nucleosomes and mapping of Fe-BABE mediated cleavage of Snf2

The 601 nucleosome positioning sequence (NPS) DNA prepared by PCR was used for nucleosome assembly. The DNA has biotin incorporated at one 5′ end and the NPS has 69 and 60 bp of flanking DNA with Gal4-binding site within the flanking 60 bp stretch (Biotin-69-601-60). Conjugation of Fe-BABE to the solvent accessible lysines in the nucleosome was done using 2-iminothiolane (2-IT) to attach a free sulfhydryl group to the accessible lysines as previously reported with some minor modifications (41, 42). Briefly, nucleosomes (0.4 uM) were incubated at 37˚C for an hr with 0.85 mM Fe-BABE and 0.425 mM 2-IT in buffer containing 10 mM MOPS pH 8, 1 mM EDTA, 5% glycerol, 0.1% NP40 and 0.5 mM PMSF. The control nucleosomes were incubated with Fe-BABE alone. Excess Fe-BABE and 2-IT were removed using a Sephadex G-50 spin column, and conjugation of Fe-BABE to the nucleosomal histones was analyzed by Western blot analysis using anti-chelate CHA225 antibody (41, 42).

Mapping of FeBABE mediated cleavage of Snf2 was performed as described previously (9). The cleavage products were analyzed by SDS-PAGE and immunoblotting using anti-HA antibody (Pierce, USA) against the C-terminal HA-tag of Snf2. Cleavage sites, and hence the nucleosome interacting regions of the SWI/SNF subunits were determined by using truncated fragments of the same protein as molecular weight standards (4).

Histone cross-linking and label transfer

Mononucleosomes (29N59) containing mutant histones with unique cysteine residues (H2A19, H2A89, H2B109 and H380) were assembled and analyzed on native PAGE with ethidium bromide staining. β-mercaptoethanol (from histone octamer) was removed by passing the assemblies through a Sephadex G-25 spin column. Sixteen nmoles of PEAS (N-(2-pyridyldithio) ethyl)-4-azidosalicylamide; a radio-iodinatable, cleavable and photoactivatible crosslinking reagent, Molecular Probes) in dimethyl sulfoxide was radiolabeled with 2.5 mCi I^{125} in a 90 µl reaction volume adjusted with 100mM sodium phosphate buffer pH 7.4. Modification was carried out in an IODO GEN (Pierce) iodination tube for 3 min at RT and stopped with 1 µl 2.5 mM tyrosine and 1 µl 80 mM methionine. Twenty pmoles of nucleosomes were modified with a 20 molar excess of iodinated PEAS for 30 min on ice. Unconjugated PEAS- I^{125} and free I^{125} were removed by passing the sample through a Sephadex G-25 spin column. The modified nucleosomes were dialyzed against final dilution buffer (10 mM Tris-HCl pH 7.5, 1 mM EDTA, 0.01% NP-40, 5% glycerol). The unmodified and modified nucleosomes were run on 4% native gel and ethidium bromide stained. WT or mutant SWI/SNF complexes were bound to the modified nucleosomes, incubated at 30°C for 30 min and the bound products separated on a 4% native polyacrylamide gel (acrylamide:bisacrylamide=36:1) at 200 V in 0.5X Tris-Borate-EDTA at 4°C. SWI/SNF bound to nucleosomes was crosslinked by UV irradiation. “Plus ATP” samples were first prebound at 30°C for 30

min and then 800μM ATP was added for 10 min before nucleosome remodeling was stopped by UV irradiation. DTT was added to a final concentration of 100 mM to reduce disulfide bonds and transfer the ^{125}I label to the crosslinked target protein. The samples were loaded on a 4-20% SDS-PAGE and radiolabeled subunits identified by phosphorimaging.

Results

The ATPase and SnAC domains of Snf2 associate with the histone portion of the nucleosome

The interactions of SWI/SNF with the histone octamer were mapped by targeted proteolysis to identify the domain(s) that anchor SWI/SNF to the nucleosome and facilitate in creating an effectively higher pulling force. Fe-BABE (Fe(III) (*S*)-1-(*p*-Bromoacetamido-benzyl)ethylene diamine tetraacetic acid), an Fe-EDTA derivative, was covalently linked to the lysine residues on the nucleosome surface including histone tails using 2-iminothiolane or 2-IT (41, 42). Fe-BABE developed by Claude Meares and colleagues (7, 8) can be used to create hydroxyl free radicals that cleave peptide binds. The extent of Fe-BABE conjugated to histones was assessed by immunoblotting using chelate specific CHA255 antibody (Fig. 1B). Modification of the histones had no apparent effect on SWI/SNF binding to nucleosomes as shown by gel shift assay (data not shown). Fe-BABE modified nucleosomes were bound to WT SWI/SNF and cleavage initiated by adding H_2O_2 and ascorbate. SWI/SNF used in these experiments had a hemagglutinin epitope (HA) tag at the C-terminus of Snf2 and immunoblotting detected full length and proteolytic fragments containing the C-terminal end of Snf2 (9). Accurate determination of the cleavage sites was done using C-terminal HA epitope tagged Snf2 polypeptides prepared by in vitro translation for size markers. Cleavage sites were mapped within a ~10 amino acid region as shown previously (4). The SnAC and ATPase domains were both found to be in close proximity to histones. Snf2 was cleaved by modified histones near amino acid residues 810, 1098, and 1342 (Fig. 1A lanes 2, 3, 5, and 6 and Fig. 1C,

black arrows). The main Snf2 cleavage site was at amino acid 810 and is located in the N-terminal lobe of the ATPase domain between motifs I and Ia. The second, relatively weaker cleavage site was at amino acid ~1098 and is in the C-terminal lobe close to motif IV (11). These two cleavage sites flank a region previously shown to be crosslinked to nucleosomal DNA 17 and 18 bp from the dyad axis (9) and are consistent with SWI/SNF binding to nucleosomes (Fig. 1D). The third cleavage site was at amino acid ~1342 located inside the SnAC domain. Cleavage at these three sites within Snf2 was dependent on modification of the accessible lysines as seen when 2-IT is omitted (Fig. 1A compare lanes 2-3 with 8-9). Also, no cleavage was observed when ascorbate and hydrogen peroxide were omitted (Fig. 1A compare lanes 1-2 or lanes 4-5). These contacts were not changed upon remodeling as shown with the addition of ATP and are consistent with these interactions being maintained during nucleosome movement (Fig. 1A compare lanes 2-3 or lanes 5-6). The addition of Gal4-VP16 did not significantly alter the contacts of Snf2 with the nucleosomal histones although cleavage around amino acid 1098 appeared to slightly stronger (Fig. 1A compare lanes 2-3 with lanes 5-6). The interactions of SWI/SNF with free DNA has been previously investigated in a similar manner by tethering Fe-BABE to DNA and is summarized in Figure 1C (9). Cleavage at the SnAC domain is specific for nucleosomes and modified histones, and is not observed when SWI/SNF binds to free DNA only. These data highlight that the likely target for the SnAC domain is histone proteins when SWI/SNF is bound to nucleosomes.

Absence of the SnAC domain reduces binding of SWI/SNF to the open histone octamer face of nucleosomes.

Another approach was used to find if the interactions of SWI/SNF with the histone octamer face are perturbed when the SnAC domain is absent. Unique cysteines were engineered into four locations on the histone octamer surface (Fig. 2A) and were designed to not perturb nucleosome structure/stability, their ability to be remodeled, and were previously used for site-directed histone photocrosslinking (10).

The SnAC domain was found to be required for stable binding of Snf2 to the histone portion of nucleosomes in the absence of ATP as there was a 2 -3 fold reduction in Snf2 cross-linking at all four positions when the SnAC domain was removed (Fig. 2B-E). The interactions of the Snf5 and Swp82 subunits of SWI/SNF were also reduced upon deletion of the SnAC domain (Fig. 2D & 2E). Remodeling decreased the extent of Snf2 and Snf5 crosslinking at residues 19 and 113 of H2A to levels similar to the reduction observed when the SnAC domain was removed (Fig 2C and 2D, compare open bars to bars with the different shades of gray). Remodeling only weakly decreased or not at all Snf2, Snf5, and Swp82 crosslinking at residue 109 of H2B and residue 80 of H3. The SnAC domain as shown by histone cross-linking has a general role in establishing the interactions between SWI/SNF and the histone octamer face of nucleosome. Taken together, these data indicate that the SnAC domain interacts with the histone portion of nucleosomes and stabilizes SWI/SNF binding to histones.

Snf2 remains in contact with nucleosomal DNA in the absence of the SnAC domain

A histone anchor domain in SWI/SNF may or may not influence the binding of the complex to nucleosomal DNA. Previously Snf2 was found to contact nucleosomal DNA at superhelical location 2 (SHL2) by site-directed DNA cross-linking and to translocate on DNA from SHL2 in a 3´ to 5´ direction (10, 45). Potential changes or loss of Snf2 interactions with nucleosomal DNA due to deletion of the SnAC domain were determined by site-directed DNA photocrosslinking. Every ~5th bp in nucleosomal DNA corresponding to positions facing in or away from the histone octamer core and every 3rd bp in extranucleosomal DNA were scanned by DNA cross-linking. The precise location of the phosphate backbone in regards to its position near the histone octamer had been previously determined for the 601 nucleosome by hydroxyl radical footprinting(18). The photoreactive group is attached to the phosphate backbone and probes contacts both in the major and minor grooves of DNA(25-27). After UV irradiation a radiolabel is transferred to the crosslinked subunit by enzymatic digestion of DNA and the

subunit identified by SDS-PAGE and phosphorimaging. WT or ΔSnAC SWI/SNF was recruited by Gal4-VP16 onto mononucleosome substrates. Snf2 was crosslinked most efficiently 17 bp from the dyad axis with WT SWI/SNF and corresponds to a position pointing in towards the histone octamer (Fig. 3A-C). Peptide mapping studies of the cross-linked Snf2 subunit suggest the ATPase C terminal lobe (between motifs IVa and V) wedges in between the DNA and histone surface at this location (9). The other two positions next to bp -17 face away from the histone octamer at bp -22 and -11, and are less efficiently cross-linked (Figure 3B). Generally, Snf2 is cross-linked to ~3 helical turns of DNA from bp -33 to 0 and is centered at the SHL2 position. Except for two positions towards the entry site at bp +52 and +63 on the side of nucleosomal DNA facing away from the histone octamer, Snf2 is not significantly cross-linked to DNA elsewhere in the nucleosome and is highly localized.

Snf2 is associated with nucleosomal DNA at the SHL2 position in ΔSnAC SWI/SNF as seen by efficient DNA crosslinking of Snf2 at bp -17 and -33 comparable to WT SWISNF (Figure 3B & 3C). There are however differences in the DNA cross-linking pattern indicating that the manner in which Snf2 is bound is altered. The most notable difference is the additional positions to which Snf2 is efficiently cross-linked to DNA with ΔSnAC SWI/SNF. Only with ΔSnAC SWI/SNF was there relatively strong cross-linking of Snf2 inside at bp -38 and others on the exposed surface of nucleosomal DNA at bp 0 and +42 (Fig. 3B and 3C). These data suggest that the binding of Snf2 to nucleosome DNA in the nucleosome is broadened in the absence of the SnAC domain and potentially has greater flexibility to scan additional proximal DNA sites. Given that ΔSnAC SWI/SNF retains contact with nucleosomal DNA, it should be able to hydrolyze ATP and translocate on DNA, but may not be able to mobilize nucleosomes without a histone anchor.

Lack of SnAC domain uncouples nucleosome mobilization from ATP hydrolysis and DNA translocation

We examined if loss of the SnAC domain caused an uncoupling of nucleosome mobilization from ATP hydrolysis. Previously ΔSnAC SWI/SNF was shown to hydrolyze ATP 7-8 fold less than WT (31) and in order to better assess remodeling differences separate from that of ATP hydrolysis, higher ATP was used with ΔSnAC SWI/SNF (320 μM) than wild type SWI/SNF (4 μM). Under these conditions the rate of hydrolysis was ~2 times faster for ΔSnAC than wild type SWI/SNF (Fig. 4A, 1.2 vs. 0.65 nM s^{-1} for ΔSnAC vs. WT). Nucleosome remodeling was followed by measuring changes in the electrophoretic mobility of nucleosomes caused by their shifting positions on DNA. Under these conditions favoring ΔSnAC SWI/SNF, the wild type SWI/SNF remodeled nucleosomes about 120 times more efficiently (Fig. 4C-D, 26 pMs^{-1} vs. 0.21 pMs^{-1} and Table 1) as determined by EMSA. The approximate number of ATP hydrolyzed per remodeling event by ΔSnAC SWI/SNF was on average 5700 as determined from the rate of ATP hydrolysis (1.2 nM s^{-1}) divided by the rate of remodeling (0.21 pM s^{-1}) and in comparison, WT SWI/SNF hydrolyzed about 25 ATP per remodeling event (0.65 nM ATP s^{-1} vs. 0.026 nM nucleosome s^{-1}). This implies that WT SWI/SNF was 270 times more efficient at converting ATP hydrolysis into nucleosome movement. Nucleosome remodeling was also assayed by restriction enzyme (RE) accessibility that measures the relative rates of nucleosomal DNA cleavage due to site exposure (Polach and Widom, 1995). Cleavage of the HhaI site near the dyad axis was monitored over time with WT and ΔSnAC SWI/SNF using the same conditions mentioned before. Exposure of the HhaI site is due to formation of DNA bulges on the surface of the nucleosomes and/or nucleosome movement away from its original position. The extent of site exposure with the ΔSnAC complex was ~64 times lower than with the WT complex (Table 1, 4.5 vs 0.07 pM DNA cut s^{-1} for WT vs ΔSnAC), which is comparable to the reduction in nucleosome movement observed by EMSA (data not shown).

The uncoupling of ATP hydrolysis from nucleosome movement could be due to defects in DNA translocation such as that observed for mutations in motif V of the ATPase domain (35). Single DNA

molecules with one end tethered to a glass slide and the other to a magnetic bead (Fig. 5A) were used to directly examine the rate of DNA translocation of both ΔSnAC and wild type SWI/SNF as previously reported for RSC (22). The height of the bead was recorded at different tension forces lower than 2 pN in the presence of ATP with and without SWI/SNF. DNA was observed to be shortened with SWI/SNF and ATP due to translocation of SWI/SNF and formation of DNA loops (Fig. 5B and 5C) as reported previously (44). ATP concentration was varied from 0.2 μM to 10 mM and the maximum rate of DNA translocation observed was at ≥1 mM ATP (data not shown). In the absence of protein, the DNA molecules undergo restricted Brownian fluctuations as expected (data not shown). SWI/SNF was recruited to a unique location on the 2.88 kb DNA fragment by Gal4-VP16 binding to two adjacent sites in the middle of the DNA template (9, 10). The recruitment of SWI/SNF by Gal4-VP16 made it possible to observe more DNA translocation events mediated by SWI/SNF at higher tension forces, where thermal fluctuations could be further suppressed and allow for shorter translocation events to be resolved. The selective recruitment of SWI/SNF by Gal4-VP16 was demonstrated with DNA shortening by SWI/SNF being dependent on Gal4-VP16 when competitor DNA was present (data not shown). Recruitment of SWI/SNF by Gal4-VP16 did not increase the force required to stall translocation by SWI/SNF.

We repeated the same magnetic tweezers experiment with the ΔSnAC SWI/SNF and observed transient shortening of DNA length similar to that for wild type SWI/SNF. Changes in DNA extension greater than the maximum height change induced by Brownian motion (determined in the absence of protein) were analyzed in order to compare the extent and rate of translocation of WT or ΔSnAC SWI/SNF on free DNA. The signal was smoothed with a rolling average of one second. The peaks with drops greater than peak drops due to Brownian fluctuations were identified with MatLab. Once a translocation event or spike was identified and the magnitude determined, the rate of translocation or velocity was fit using straight lines as shown in Figure 5C. We found that at 0.3pN, the average loop size on DNA is 580 ± 20

bp for WT and 550 ± 70 for ΔSnAC (Fig. 5D and Table 1). The force dependence of DNA shortening for both WT and ΔSnAC SWI/SNF are very similar as shown in Figure 5D. At 0.3 pN, we found the rate of translocation is 600 ± 100 bp/s for WT and 500 ± 100 for ΔSnAC (Fig. 5E and Table 1). Single molecule measurements showed mutants lacking the SnAC domain have the same average loop size and translocate at the same rate as WT along duplex DNA and therefore the SnAC domain is not required for SWI/SNF translocation along duplex DNA.

The SnAC domain is essential for translocation on nucleosomal templates

A similar setup was used to examine the rate of nucleosome movement and DNA translocation in a nucleosomal context. The same DNA template as before containing a 601 nucleosome positioning sequence was used to reconstitute and position a single nucleosome on DNA. SWI/SNF translocation of nucleosomes and shortening of DNA tolerate significantly higher tension forces than translocation of SWI/SNF on free DNA as shown previously (44). A single nucleosome was observed to be bound to each DNA as the change in end-to-end distances observed when adjusting the tension force from 0.3 to 26 pN corresponding to that expected for unwrapping one nucleosome from DNA (data not shown). Changes in DNA length were observed at 3 pN when WT SWI/SNF and ATP were added as observed with shortening of the end-to-end distances, but no shortening was observed with ΔSnAC SWI/SNF (Fig. 5F). In 13 of 15 traces there was clear evidence of DNA shortening with WT SWI/SNF, but in 13 traces with ΔSnAC SWI/SNF no DNA shortening was observed. There was no inherent problem with these templates as shown by WT and ΔSnAC SWI/SNF being able to equally translocate along the free DNA portion of the template when the tension force was reduced to 0.3 pN (data not shown). Single molecule experiments show that in the absence of SnAC, SWI/SNF is unable to move DNA through nucleosomes creating DNA loops and thereby shortening the DNA tether.

In order to examine more carefully the molecular changes in DNA and histone interactions associated with nucleosome movement, we monitored the interactions of residue 45 of histone H2A with DNA before and during remodeling. Alanine 45 of histone H2A was changed to a cysteine and conjugated to an aryl azide for probing these interactions. After crosslinking to DNA, the DNA site is labile under alkaline conditions and the cleavage site mapped with base pair resolution. Residue 45 is close to nucleosomal DNA 37 and 39 bp from the dyad axis and in one of its two orientations is ~15 bp from where the ATPase domain of Snf2 is normally bound (9, 20). SWI/SNF was bound to nucleosomes and the position most proximal to the ATPase domain binding site monitored. WT SWI/SNF moved nucleosomes away from the original position as monitored by reduction of cutting at bp -37 with almost half having moved after 10 s and nearly completely moved after 160 s (Fig. 6A and 6B). Within 10 seconds, the crosslinked site was shifted to bp -87 and is 50 bp from its original position placing the edge of the nucleosome 22 bp past the DNA end. Later after 40 seconds, a new crosslinked position was also seen at bp +72 that represents a 110 bp step to the other side with the longer extranucleosomal DNA, placing the nucleosome 49 bp off the other edge of DNA (Fig. 6B). ΔSnAC SWI/SNF did not significantly move DNA inside nucleosomes from its original position and there doesn't appear to be any significant movement of nucleosomal DNA ~15 bp away from where the ATPase domain is likely bound (Fig. 6C). Even limited movement of nucleosomal DNA is not observed without the SnAC domain of SWI/SNF. Given that Snf2 is still bound to nucleosomal DNA, hydrolyzes ATP, and can equally well translocate along DNA without the SnAC domain; it is very significant that nonetheless it is unable to move DNA inside the nucleosome ~15 bp from where the ATPase domain is bound. These data highlight the critical importance of a histone anchor in SWI/SNF to facilitate in the initial movement of DNA inside of nucleosomes.

Discussion

Converting ATP hydrolysis and DNA translocation by SWI/SNF into nucleosome movement requires the SnAC domain to bind to histones

Deletion of the SnAC domain of Snf2 uncouples ATP hydrolysis and DNA translocation by SWI/SNF from nucleosome mobilization. The SnAC domain is evolutionary conserved in all eukaryotic SWI/SNF complexes and is essential for the in vitro and in vivo activity of SWI/SNF (31). Although SnAC enhances ATP hydrolysis by SWI/SNF, its role is more pronounced for being required to convert ATP hydrolysis and DNA translocation into changes of nucleosome translational positions. The two roles of SnAC are distinguished from each other by using different concentrations of ATP with each in order to have equivalent rates of ATP hydrolysis with wild type SWI/SNF and SWI/SNF lacking the SnAC domain. Even when ΔSnAC SWI/SNF hydrolyzed ATP two times faster than wild type SWI/SNF, ΔSnAC SWI/SNF moved nucleosomes ~120 times slower than wild type SWI/SNF. The extent and type of uncoupling shown for the SnAC domain has never been observed before to our knowledge for any ATP-dependent chromatin remodeler. Most uncoupling of chromatin remodelers are generally only <5 times that of wild type and involve a reduction in DNA translocation compared to ATP hydrolysis. Previously, mutations in motif V of the ATPase domain of SWI/SNF have uncoupled ATP hydrolysis from DNA translocation (17, 24, 35, 43). These mutations are in a motif that is conserved in multiple DNA helicases and in some of these instances this motif has been shown to directly interact with DNA. Changes in motif V of Snf2 probably uncouple ATP hydrolysis from DNA translocation by causing the enzyme to hold less tightly to DNA. Loss of the SnAC domain however does not have this effect as ΔSnAC SWI/SNF translocates on single DNA molecules with rates and total distances traversed comparable to wild type SWI/SNF. Besides mutations within the ATPase domain, a domain outside of the ATPase domain known as the HSA domain when removed reduces remodeling efficiency about a factor of <2 (38). The HSA domain binds to the actin related proteins Arp 7 and 9 that are shared between RSC and SWI/SNF. The HSA domain likely stimulates chromatin remodeling through the interaction of the Arp 7 and 9 subunits (2, 28, 39). The

469 HSA domain also has a propensity to bind to free DNA, which may also enhance the remodeling
470 activities of RSC and SWI/SNF (9). The SnAC domain unlike the HSA domain does not bind or recruit
471 other subunits to the SWI/SNF complex or bind DNA like the HSA domain and seems to have a very
472 different target.
473
474 **The SnAC domain is a histone anchor required to create sufficient force to mobilize nucleosomes**
475 SWI/SNF requires a stable anchor to create a sufficient pulling force to move nucleosomes when the
476 ATPase is bound at SHL2. The strong uncoupling of ATP hydrolysis and DNA translocation from
477 nucleosome movement when the SnAC domain is removed is characteristic of a crucial histone anchor.
478 The SnAC domain satisfies several of the criteria expected for a histone anchor of SWI/SNF. First and
479 foremost SnAC appears to bind to the histone component of nucleosomes as shown by an innovative
480 protein footprinting technique using an artificial protease tethered to the histones in nucleosomes. The
481 only other domain shown to interact in this manner is the ATPase domain. Consistent with this finding
482 is the observation that when SnAC is missing the interactions of SWI/SNF with the open histone octamer
483 face of the nucleosome are reduced overall as seen by site-directed crosslinking. These effects are
484 specific to histones as Snf2 is still observed to bind well to nucleosomal DNA as would be expected for a
485 histone anchor domain that uncouples DNA translocation from moving nucleosomes. In support of our
486 work, when switching the ATPase-helicase domains between BRG1 and SNF2h, a region from residue
487 1250-1386 of BRG1 including the SnAC domain was required in addition to the ATPase domain to retain
488 the remodeling activity of any BRG1 chimeras(13). In another study, a region from amino acid 1223-1420
489 from BRG1 encompassing the SnAC domain (residues 1332-1390) was found to be essential for
490 remodeling and histone H3 interactions (21). These data show the SnAC domain is important for
491 regulating SWI/SNF activity in both yeast and humans. The other criteria is that SnAC is exquisitely
492 required for SWI/SNF to move nucleosomal DNA even short distances from their original positions when

proximal to the bound ATPase domain. This was shown using a method to track changes in histone-DNA interactions with base pair resolution 37 bp from the dyad axis.

Our model for the SnAC domain is that it binds to the histone octamer and provides an anchor for the ATPase domain (Fig. 7). This anchor is required for the ATPase domain to gain traction and create a sufficient pulling force to move DNA inside of nucleosomes. Just like a Tet-dimer fused to the Sth1 catalytic subunit converts it from being able to create a pulling force of ~1 pN to a pulling force of almost 30 pN (34), SnAC domain as an anchor also can make the ATPase domain of Snf2 to have a significantly higher pulling force. Thus the pulling force of a chromatin remodeler may be more a function of the strength of its anchor to the nucleosomes rather than the strength of the ATPase domain alone. It will be important to find how other chromatin remodelers interact with nucleosomes and potentially have key anchors like SWI/SNF or not. Histone anchors like that observed for SWI/SNF may be more a function of those remodelers that disassemble nucleosomes rather than of those remodelers involved in changing nucleosome spacing.

Acknowledgements

This work was supported by NIH grant GM 48413 to B.B., a Career Award from Burroughs Wellcome Fund to M.G.P., by NIH grant GM 083055 to M.G.P.; and an American Heart Association postdoctoral fellowship 12POST9380003 to P.V.

We would like to thank Nilanjana Chatterjee for help with the DNA photoaffinity labeling experiments, Dr. Claude Meares for providing CHA225 antibodies, Kimberly Dimauro for help with single molecule experiments and Dr. Robert Forties for calculating the end-to-end distance distribution of a worm-like chain.

References

1. **Brower-Toland, B. D., C. L. Smith, R. C. Yeh, J. T. Lis, C. L. Peterson, and M. D. Wang.** 2002. Mechanical disruption of individual nucleosomes reveals a reversible multistage release of DNA. Proc Natl Acad Sci U S A **99:**1960-5.

2. **Cairns, B. R., H. Erdjument-Bromage, P. Tempst, F. Winston, and R. D. Kornberg.** 1998. Two actin-related proteins are shared functional components of the chromatin-remodeling complexes RSC and SWI/SNF. Mol Cell **2:**639-51.

3. **Chatterjee, N., D. Sinha, M. Lemma-Dechassa, S. Tan, M. A. Shogren-Knaak, and B. Bartholomew.** Histone H3 tail acetylation modulates ATP-dependent remodeling through multiple mechanisms. Nucleic Acids Res **39:**8378-91.

4. **Chen, H. T., and S. Hahn.** 2003. Binding of TFIIB to RNA polymerase II: Mapping the binding site for the TFIIB zinc ribbon domain within the preinitiation complex. Mol Cell **12:**437-47.

5. **Clapier, C. R., and B. R. Cairns.** 2009. The biology of chromatin remodeling complexes. Annu Rev Biochem **78:**273-304.

6. **Dang, W., and B. Bartholomew.** 2007. Domain architecture of the catalytic subunit in the ISW2-nucleosome complex. Mol Cell Biol **27:**8306-17.

7. **Datwyler, S. A., and C. F. Meares.** 2001. Artificial iron-dependent proteases. Met Ions Biol Syst **38:**213-54.

8. **Datwyler, S. A., and C. F. Meares.** 2000. Protein-protein interactions mapped by artificial proteases: where sigma factors bind to RNA polymerase. Trends Biochem Sci **25:**408-14.

9. **Dechassa, M. L., S. K. Hota, P. Sen, N. Chatterjee, P. Prasad, and B. Bartholomew.** 2012. Disparity in the DNA translocase domains of SWI/SNF and ISW2. Nucleic Acids Res.

10. **Dechassa, M. L., B. Zhang, R. Horowitz-Scherer, J. Persinger, C. L. Woodcock, C. L. Peterson, and B. Bartholomew.** 2008. Architecture of the SWI/SNF-Nucleosome Complex. Mol Cell Biol.

11. **Durr, H., C. Korner, M. Muller, V. Hickmann, and K. P. Hopfner.** 2005. X-ray structures of the Sulfolobus solfataricus SWI2/SNF2 ATPase core and its complex with DNA. Cell **121:**363-73.

12. **Fairman-Williams, M. E., U. P. Guenther, and E. Jankowsky.** SF1 and SF2 helicases: family matters. Curr Opin Struct Biol **20:**313-24.

13. **Fan, H. Y., K. W. Trotter, T. K. Archer, and R. E. Kingston.** 2005. Swapping function of two chromatin remodeling complexes. Mol Cell **17:**805-15.

14. **Gangaraju, V. K., and B. Bartholomew.** 2007. Mechanisms of ATP dependent chromatin remodeling. Mutat Res **618:**3-17.

15. **Gorbalenya, A. E., E. V. Koonin, A. P. Donchenko, and V. M. Blinov.** 1989. Two related superfamilies of putative helicases involved in replication, recombination, repair and expression of DNA and RNA genomes. Nucleic Acids Res **17:**4713-30.

16. **Hota, S. K., and B. Bartholomew.** 2011. Diversity of operation in ATP-dependent chromatin remodelers. Biochim Biophys Acta **1809:**476-87.

17. **Hsu, D. S., S. T. Kim, Q. Sun, and A. Sancar.** 1995. Structure and function of the UvrB protein. J Biol Chem **270:**8319-27.

18. **Kagalwala, M. N., B. J. Glaus, W. Dang, M. Zofall, and B. Bartholomew.** 2004. Topography of the ISW2-nucleosome complex: insights into nucleosome spacing and chromatin remodeling. EMBO J **23:**2092-104.

19. **Kassabov, S. R., N. M. Henry, M. Zofall, T. Tsukiyama, and B. Bartholomew.** 2002. High-resolution mapping of changes in histone-DNA contacts of nucleosomes remodeled by ISW2. Mol Cell Biol **22:**7524-34.

20. **Kassabov, S. R., B. Zhang, J. Persinger, and B. Bartholomew.** 2003. SWI/SNF unwraps, slides, and rewraps the nucleosome. Mol Cell **11:**391-403.

21. **Lavigne, M., R. Eskeland, S. Azebi, V. Saint-Andre, S. M. Jang, E. Batsche, H. Y. Fan, R. E. Kingston, A. Imhof, and C. Muchardt.** 2009. Interaction of HP1 and Brg1/Brm with the globular domain of histone H3 is required for HP1-mediated repression. PLoS Genet **5:**e1000769.

22. **Lia, G., E. Praly, H. Ferreira, C. Stockdale, Y. C. Tse-Dinh, D. Dunlap, V. Croquette, D. Bensimon, and T. Owen-Hughes.** 2006. Direct observation of DNA distortion by the RSC complex. Mol Cell **21:**417-25.

23. **Luger, K., T. J. Rechsteiner, and T. J. Richmond.** 1999. Preparation of nucleosome core particle from recombinant histones. Methods Enzymol **304:**3-19.

24. **Moolenaar, G. F., R. Visse, M. Ortiz-Buysse, N. Goosen, and P. van de Putte.** 1994. Helicase motifs V and VI of the Escherichia coli UvrB protein of the UvrABC endonuclease are essential for the formation of the preincision complex. J Mol Biol **240:**294-307.

25. **Naryshkin, N., Y. Kim, Q. Dong, and R. H. Ebright.** 2001. Site-specific protein-DNA photocrosslinking. Analysis of bacterial transcription initiation complexes. Methods Mol Biol **148:**337-61.

26. **Persinger, J., and B. Bartholomew.** 1996. Mapping the contacts of yeast TFIIIB and RNA polymerase III at various distances from the major groove of DNA by DNA photoaffinity labeling. J Biol Chem **271:**33039-46.

588 27. **Persinger, J., and B. Bartholomew.** 2009. Site-directed DNA crosslinking of large
589 multisubunit protein-DNA complexes. Methods Mol Biol **543:**453-74.

590 28. **Peterson, C. L., Y. Zhao, and B. T. Chait.** 1998. Subunits of the yeast SWI/SNF
591 complex are members of the actin-related protein (ARP) family. J Biol Chem **273:**23641-
592 4.

593 29. **Saha, A., J. Wittmeyer, and B. R. Cairns.** 2002. Chromatin remodeling by RSC
594 involves ATP-dependent DNA translocation. Genes Dev **16:**2120-34.

595 30. **Saha, A., J. Wittmeyer, and B. R. Cairns.** 2005. Chromatin remodeling through
596 directional DNA translocation from an internal nucleosomal site. Nat Struct Mol Biol
597 **12:**747-55.

598 31. **Sen, P., S. Ghosh, B. F. Pugh, and B. Bartholomew.** 2011. A new, highly conserved
599 domain in Swi2/Snf2 is required for SWI/SNF remodeling. Nucleic Acids Res.

600 32. **Sengupta, S. M., J. Persinger, B. Bartholomew, and C. L. Peterson.** 1999. Use of
601 DNA photoaffinity labeling to study nucleosome remodeling by SWI/SNF. Methods
602 **19:**434-46.

603 33. **Singleton, M. R., M. S. Dillingham, and D. B. Wigley.** 2007. Structure and mechanism
604 of helicases and nucleic acid translocases. Annu Rev Biochem **76:**23-50.

605 34. **Sirinakis, G., C. R. Clapier, Y. Gao, R. Viswanathan, B. R. Cairns, and Y. Zhang.**
606 2011. The RSC chromatin remodelling ATPase translocates DNA with high force and
607 small step size. EMBO J **30:**2364-72.

608 35. **Smith, C. L., and C. L. Peterson.** 2005. A conserved Swi2/Snf2 ATPase motif couples
609 ATP hydrolysis to chromatin remodeling. Mol Cell Biol **25:**5880-92.

610 36. **Strick, T. R., J. F. Allemand, D. Bensimon, A. Bensimon, and V. Croquette.** 1996.
611 The elasticity of a single supercoiled DNA molecule. Science **271:**1835-7.

612 37. **Strick, T. R., J. F. Allemand, D. Bensimon, and V. Croquette.** 1998. Behavior of
613 Supercoiled DNA. Biophysical journal **74:**2016-2028.

614 38. **Szerlong, H., K. Hinata, R. Viswanathan, H. Erdjument-Bromage, P. Tempst, and**
615 **B. R. Cairns.** 2008. The HSA domain binds nuclear actin-related proteins to regulate
616 chromatin-remodeling ATPases. Nat Struct Mol Biol **15:**469-76.

617 39. **Szerlong, H., A. Saha, and B. R. Cairns.** 2003. The nuclear actin-related proteins Arp7
618 and Arp9: a dimeric module that cooperates with architectural proteins for chromatin
619 remodeling. EMBO J **22:**3175-87.

620 40. **Thastrom, A., P. T. Lowary, and J. Widom.** 2004. Measurement of histone-DNA
621 interaction free energy in nucleosomes. Methods **33:**33-44.

41. **Traviglia, S. L., S. A. Datwyler, and C. F. Meares.** 1999. Mapping protein-protein interactions with a library of tethered cutting reagents: the binding site of sigma 70 on Escherichia coli RNA polymerase. Biochemistry **38:**4259-65.

42. **Traviglia, S. L., S. A. Datwyler, D. Yan, A. Ishihama, and C. F. Meares.** 1999. Targeted protein footprinting: where different transcription factors bind to RNA polymerase. Biochemistry **38:**15774-8.

43. **Velankar, S. S., P. Soultanas, M. S. Dillingham, H. S. Subramanya, and D. B. Wigley.** 1999. Crystal structures of complexes of PcrA DNA helicase with a DNA substrate indicate an inchworm mechanism. Cell **97:**75-84.

44. **Zhang, Y., C. L. Smith, A. Saha, S. W. Grill, S. Mihardja, S. B. Smith, B. R. Cairns, C. L. Peterson, and C. Bustamante.** 2006. DNA translocation and loop formation mechanism of chromatin remodeling by SWI/SNF and RSC. Mol Cell **24:**559-68.

45. **Zofall, M., J. Persinger, S. R. Kassabov, and B. Bartholomew.** 2006. Chromatin remodeling by ISW2 and SWI/SNF requires DNA translocation inside the nucleosome. Nat Struct Mol Biol **13:**339-46.

Figure Legends

***Figure 1*. The SnAC domain associates with nucleosomal histones.**

(A) The interactions of Snf2 in the context of the whole SWI/SNF complex with nucleosomes were probed by Fe-BABE being conjugated to solvent accessible lysine residues in nucleosomes. Cleavage of Snf2 was detected by immunoblotting using an antibody against the C-terminal HA-epitope of Snf2. Nucleosomes were modified with 2-iminothiolane (2IT) and Fe-BABE (lane 1-6) or with Fe-BABE alone (lane 7-9) as a negative control. ATP (1 mM) was added in lanes 3 and 6 and incubated before addition of ascorbate and hydrogen peroxide. (B) The successful coupling of Fe-BABE to nucleosomes was detected by immunoblotting using the anti-chelate antibody CHA225. Nucleosomes were incubated with Fe-BABE alone (lane 2) or Fe-BABE and 2IT (lane 3). (C) Map of the Snf2 domains including the ATPase domain with conserved helicase motifs is shown. The other domains include the QLQ domain and HSA (helicase-SANT-associated) domain on the N terminal half and the SnAC (Snf2 ATP coupling),

652 tandem AT hooks and bromodomain in the C terminal half of Snf2. The regions of Snf2 shown to contact
653 free DNA (gray arrows) and histone octamer (black arrows) by Fe-BABE mediated proteolysis are shown.
654 The thickness of the arrows is proportional to the frequency of cleavage. (D) A structural model of the
655 ATPase domain (beige) bound to DNA (blue) based on the crystal structure of Rad54 is shown. The
656 regions shown to be close to histones by cleavage (green) or to nucleosomal DNA by crosslinking (red)
657 are highlighted.
658
659 ***Figure 2.*** **Loss of SnAC reduces interactions of SWI/SNF with the open face of the histone octamer.**
660 (A) The location of the four positions in the open face of the histone octamer inside nucleosomes used
661 to probe for the interactions of SWI/SNF are shown in magenta. A side and top view are displayed. (B)
662 Modified nucleosomes were bound to ΔSnAC (lanes 3, 5, 7 and 9) and WT SWI/SNF (lanes 2, 4, 6 and 8)
663 in the absence of ATP (B) or presence of 800μM ATP (gel not shown) . After cross-linking, the radiolabel
664 was transferred and the subunits of SWI/SNF resolved on a 4-20% SDS-PAGE. Labeled proteins were
665 detected by phosphorimaging. Lane 1 had photoreactive H380 nucleosomes, but no SWI/SNF was
666 added before cross-linking. The relative amount of Snf2 (C), Snf5 (D), and Swp82 (E) crosslinked at the
667 different histone positions for WT SWI/SNF (-ATP (black bar), + ATP (white bar)) and ΔSnAC (- ATP (dark
668 gray bar), + ATP (light gray bar)) SWI/SNF are shown. The crosslinking experiments were done in
669 triplicates and standard deviations shown.
670
671 ***Figure 3*****. Loss of the SnAC domain does not reduce the interactions of Snf2 with nucleosomal DNA.**
672 (A) SWI/SNF was recruited to nucleosomes by Gal4-VP16 binding 27 bp from the entry site of the
673 nucleosome as described in Materials and Methods. The cross-linked protein(s) were analyzed on 4-
674 20% SDS-PAGE and detected by phosphorimaging. A representative of several gels for WT (top panel,
675 lanes 1-8) and ΔSnAC SWI/SNF (bottom panel, lanes 9-16) is shown for cross-linking with nucleosomal

DNA at sites spanning from bp -17 to -54. Crosslinking of WT Snf2 at bp -17 (lanes 8 and 17) was used as the reference in all gels for normalization. (B-C) Mapping the interactions of Snf2 with DNA by DNA cross-linking was done at 27 positions along nucleosomal DNA and 10 along extranucleosomal DNA. The nucleosomal positions probed every helical turn face either in (B) or away (C) from the histone octamer. The gray closed triangles represent WT and black open squares ΔSnAC cross-linking. Every 3rd bp was probed in extranucleosomal DNA (B; gray closed diamond for WT and black closed diamond for ΔSnAC). The amount of label transferred to the Snf2 subunit was quantified and normalized to the amount of label transferred to Snf2 when cross-linked at bp -17 using WT SWI/SNF (relative cross-linking). The numbering system is relative to the nucleosomal dyad axis as zero and positions to the left being negative and those to the right being positive.

Figure 4. **The SnAC domain couples ATP hydrolysis of SWI/SNF to nucleosome movement.** The rates of ATP hydrolysis of the WT (A) and ΔSnAC SWI/SNF (B) were measured under full binding conditions with 6.4 nM 29N59 mononucleosomes (29 and 59 bp of extranucleosomal DNA) and 20 nM SWI/SNF. The ATP concentration used for WT and ΔSnAC SWI/SNF was respectively 4.4 μM and 320 μM. The time scale was also different for WT SWI/SNF (0 to 10 min) versus that for ΔSnAC SWI/SNF (0 to 120 min). (C-D) The rate of nucleosome movement by WT (lanes 1-8) and ΔSnAC SWI/SNF (lanes 9-17) was followed by gel shift assay under the same conditions as in (A) and (B). The amount of nucleosomes moved versus time for WT (closed triangle) and ΔSnAC SWI/SNF (open circle) are compared.

Figure 5**. SnAC is not required for translocation on free DNA, but is on nucleosomes.** (A) Cartoon illustrating the magnetic tweezers geometry for detecting SWI/SNF translocation events along a single DNA molecule. (B) Time traces of the end-to-end distance of a 2.88 kb DNA molecule with and without 5nM SWI/SNF. The gray points are the raw data, while the black curve is a 1 s rolling average of time series. The long spikes that correspond to DNA shortening caused by SWI/SNF (bottom

700 time trace) are not present in the absence of the SWI/SNF complex (top time trace). (C) Two of the
701 characteristic translocation events from the bottom time trace in panel B are shown. The translocation
702 rates were determined by fitting individual events using a straight line (red line). We observed two
703 distinct types of translocation events. The top time series shows an event where SWI/SNF shortens the
704 DNA end-to-end distance, stalls, and then reverses directions. The bottom time series shows an event
705 where SWI/SNF shortens the end-to-end distance and then reverses direction without any significant
706 stall time. Both type of translocation events were previously reported for RSC. (D) Force dependence of
707 DNA shortening measured at 1 mM ATP for WT (gray filled triangles) and ΔSnAC SWI/SNF (black open
708 squares) complexes. (E) Force dependence of the translocation rates for WT (gray filled triangles) and
709 ΔSnAC (black open squares) SWI/SNF. Data was taken at 1 mM ATP, in the presence of Gal4-VP16. (f)
710 Example time traces of the end-to-end distance of a 2.88 kb DNA molecule containing 1 nucleosome and
711 the flow cell contains 5 nM WT (upper trace) or ΔSnAC SWI/SNF (lower trace) and 1 mM ATP. Changes in
712 end-to-end distances were observed under a pulling force of 3 pN. A remodeling event is circled in the
713 upper trace. A total of 15 traces for WT SWI/SNF and 13 traces for ΔSnAC SWI/SNF were obtained with
714 tethers containing a single nucleosome.
715
716 ***Figure 6*. ΔSnAC SWI/SNF cannot move nucleosomal DNA close to the binding site of the ATPase**
717 **domain.**
718 (A) Nucleosome positions were mapped using site-directed crosslinking and alkali mediated cleavage at
719 different times during remodeling. The photocrosslinker was placed at residue 45 of histone H2A and
720 alkali-induced cleavage of DNA monitored with the bottom strand radiolabeled. The original cut site was
721 at bp -37 (black rectangle) and the DNA translocation site was 15-25 bp from the dyad axis (yellow
722 rectangle). Remodeling was initiated by the addition of ATP and changes in histone-DNA interactions
723 examined after 10 (red), 40 (green), and 160 s (purple). (B-C) Lane profile overlay analyses of the

724 sequencing gels from site-directed mapping experiments are shown for WT (B)and ΔSnAC (C) complexes.
725 The x and y axes denote bp position (dyad being zero, left of dyad being negative and right of dyad being
726 positive) and cross-linking/cleavage signal in arbitrary units respectively. Time-dependent decrease in
727 cross-linking/cleavage signal at the original nucleosome position is shown on the left panel. Appearance
728 of cross-linking/cleavage signal upon remodeling is shown at the -87 (middle panel) and +72 (right
729 panel) positions indicating 50bp movement towards the shorter linker and 110bp movement towards
730 the longer linker respectively. Note the lack of movement measured by either disappearance of cross-
731 linking/cleavage at the original nucleosome position or the appearance of cross-linking/cleavage at -87
732 or +72 positions in case of the ΔSnAC complex (C).
733
734 ***Figure 7*. Model for an anchor to histones being required for SWI/SNF to mobilize nucleosomes.**
735 Histone octamer is shown as a sphere with numbers indicating different superhelical positions and a
736 black line representing DNA with positions having the corresponding number. ATPase lobes are gray
737 ovals (I and II) and hinge region shown as a black line connecting the two lobes. Blue region is the SnAC
738 domain. (A) When SnAC is present the ATPase domain is anchored to the histone octamer and pulls DNA
739 through it. The ATPase domain when tethered has sufficient force to disrupt histone-DNA interactions
740 toward the entry site and create DNA bulges on the surface of nucleosomes. (B) In the absence of SnAC
741 as a histone anchor, the ATPase domain is not fixed and cannot create a sufficient pulling force to
742 disrupt histone-DNA interactions.
743
744
745

746 **Table 1: Kinetic parameters of ΔSnAC complex obtained from Michaelis-Menten analysis, remodeling**

747 **and ATPase assays**

	WT	**ΔSnAC**
Rate of remodeling (pM s^{-1})	2.6[a]	0.021[b]
Rate of ATP hydrolysis (nM s^{-1})	0.65[a] 8.3 +/- 0.35[b]	1.2 +/- 0.049[b]
# of ATP required to mobilize 1 nucleosome	25[a]	5700[b]
Rate of HhaI site exposure (pM DNA cut s^{-1})	4.5[a]	0.07[b]
Rate of DNA translocation (bp/s)	600±100	500±100
Average distance traveled on DNA (bp)	580±20	550±70
Rate of translocation on nucleosomes	100 ± 50 bp/s	n/a

748 [a]Reaction conditions 4.4uM ATP at 25ºC

749 [b]Reaction conditions 320uM ATP at 30˚C

750

751

752

753

754

755

756

757

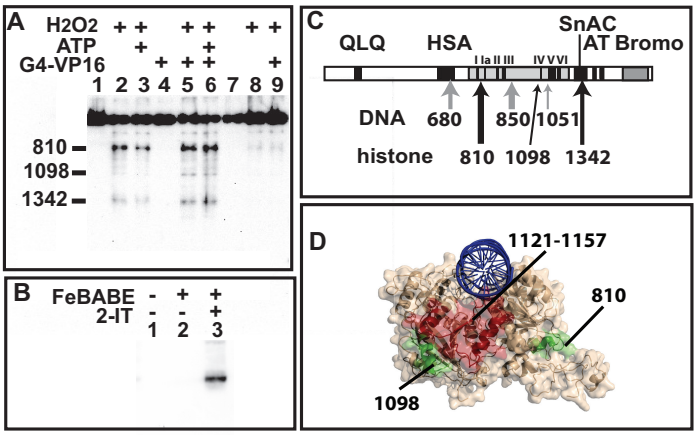

Figure 1
1.5 column width

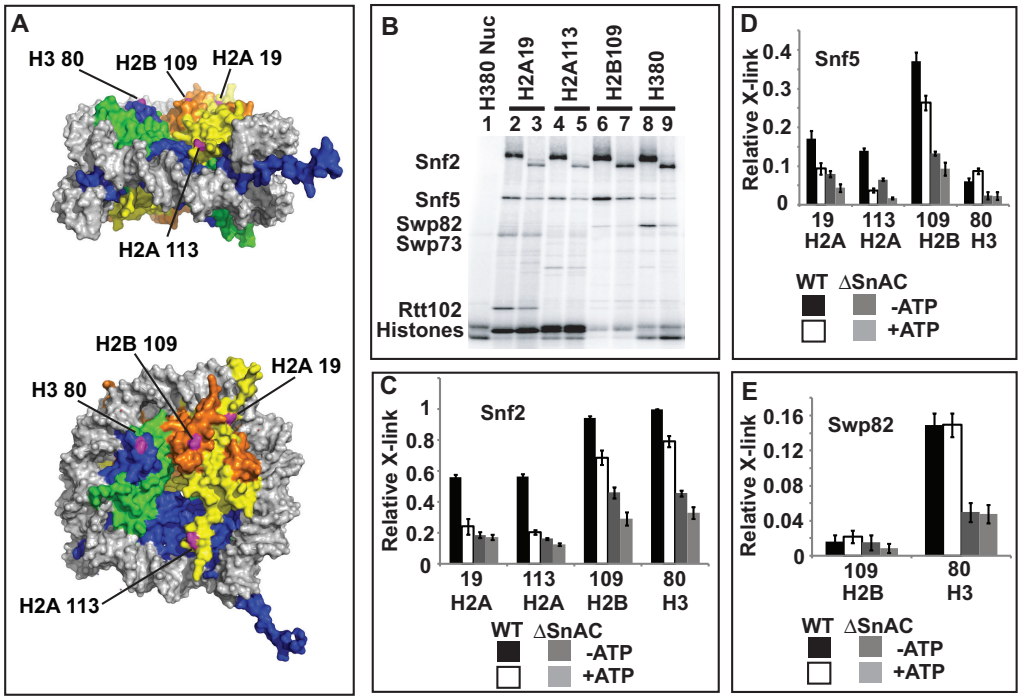

Figure 2 --2 column width

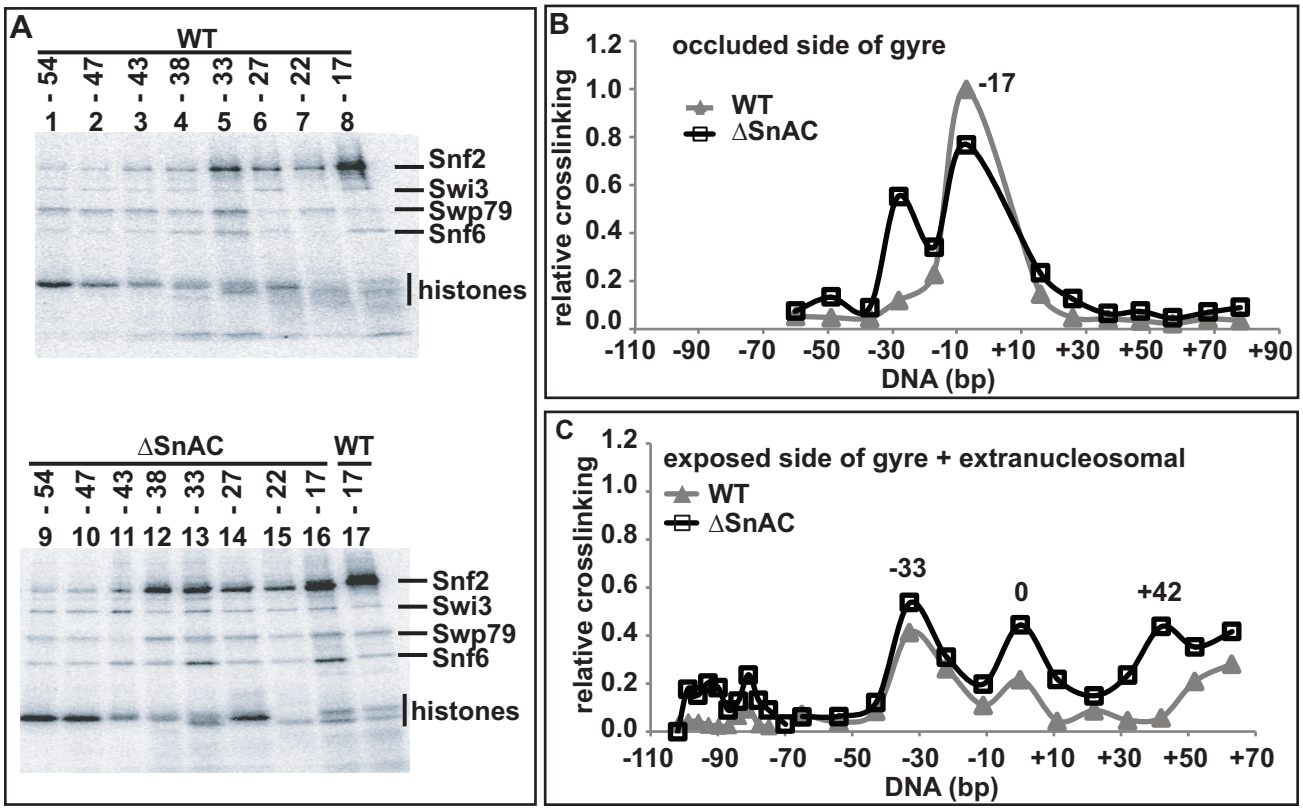

Figure 3 - 2 column width

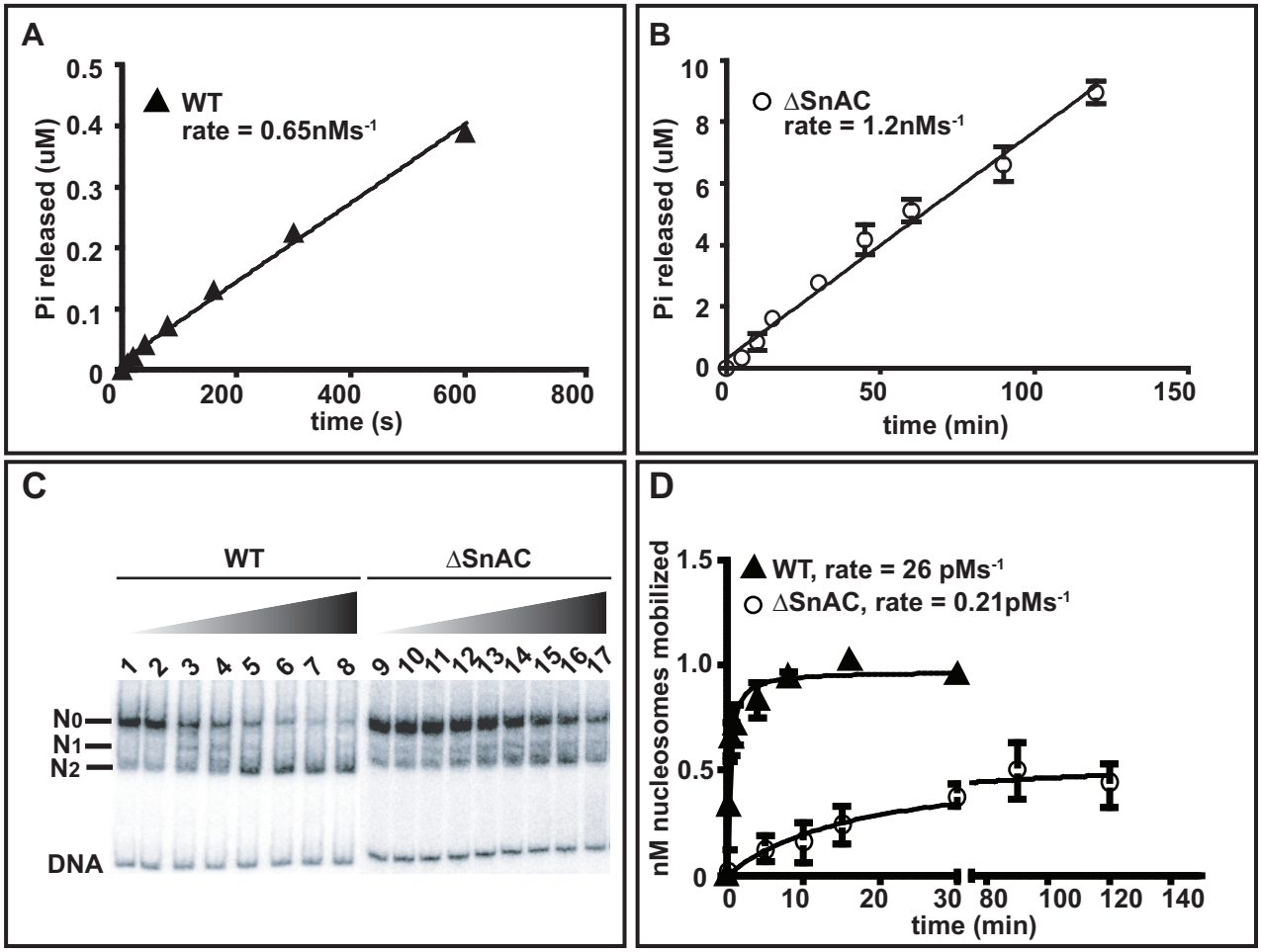

Figure 4 - 2 column width

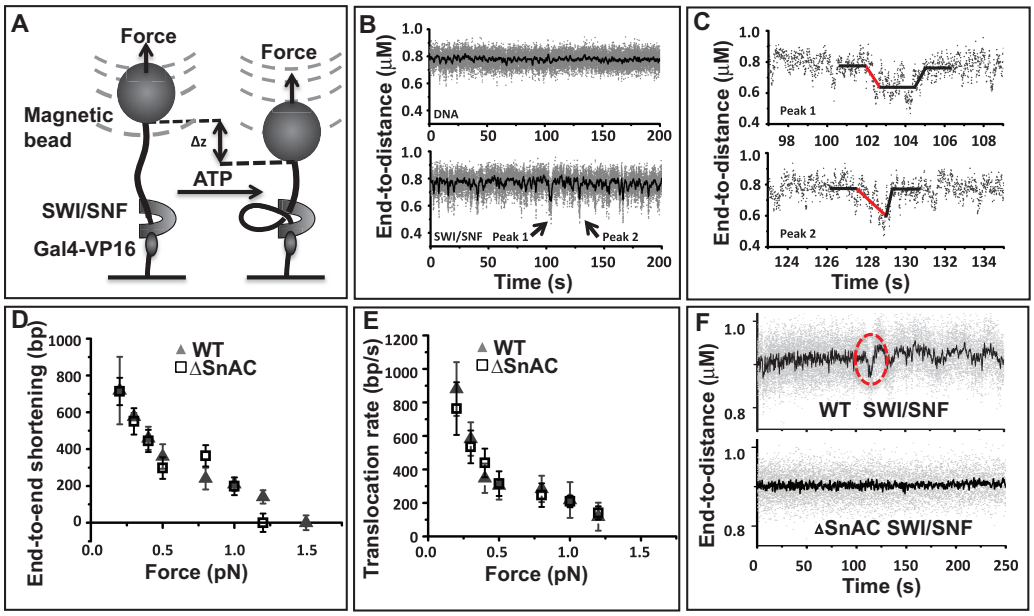

Figure 5 - 2 column width

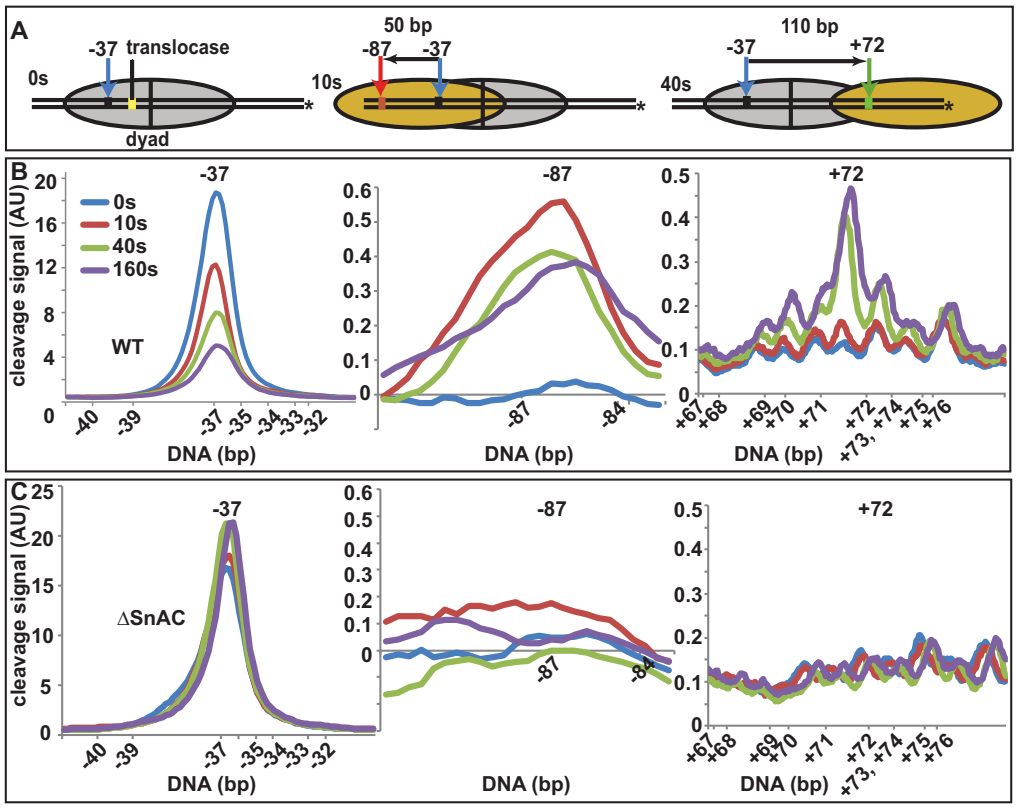

Figure 6 - 2 column width